INL/CON-12-26385
PREPRINT

Preliminary Design for Conventional and Compact Secondary Heat Exchanger in a Molten Salt Reactor

ASME 2012 Summer Heat Transfer Conference HT 2012

Piyush Sabharwall
Eung Soo Kim
Ali Siahpush
Mike Patterson

July 2012

The INL is a
U.S. Department of Energy
National Laboratory
operated by
Battelle Energy Alliance

This is a preprint of a paper intended for publication in a journal or proceedings. Since changes may be made before publication, this preprint should not be cited or reproduced without permission of the author. This document was prepared as an account of work sponsored by an agency of the United States Government. Neither the United States Government nor any agency thereof, or any of their employees, makes any warranty, expressed or implied, or assumes any legal liability or responsibility for any third party's use, or the results of such use, of any information, apparatus, product or process disclosed in this report, or represents that its use by such third party would not infringe privately owned rights. The views expressed in this paper are not necessarily those of the United States Government or the sponsoring agency.

ASME 2012 Summer Heat Transfer Conference
HT2012
July 8-12, 2012, Puerto Rico, USA

HT2012-58007

PRELIMINARY DESIGN FOR CONVENTIONAL AND COMPACT SECONDARY HEAT EXCHANGER IN A MOLTEN SALT REACTOR

Piyush Sabharwall
Idaho National Laboratory
Idaho Falls, ID USA

Eung Soo Kim
Seoul National University
Seoul, South Korea

Ali S. Siahpush
Idaho National Laboratory
Idaho Falls, ID USA

Mike Patterson
Idaho National Laboratory
Idaho Falls, ID USA

ABSTRACT

In this study, the heat transfer coolant utilized in the heat exchanger is a molten salt, which transfers thermal energy to water (steam) for power production by a supercritical Rankine (25MPa) or subcritical Rankine (17MPa) cycle. Molten salts are excellent coolants, with 25% higher volumetric heat capacity than pressurized water, and nearly five times that of liquid sodium. The greater heat capacity of molten salts results in more compact components like pumps and heat exchangers. However, the use of a molten salt provides potential materials compatibility issues. After studying a variety of individual molten salt mixtures, chlorides and fluorides have been given the most serious consideration because of their heat transport and transfer characteristics

In this study thermal designs of conventional (shell and tube), and compact (printed circuit) heat exchangers are carried out and compared for a given thermal duty. There are a couple of main issues that need to be addressed before this technology could be commercialized. The main issue is with the material compatibility of molten salts (especially fluoride salts) and secondarily, with the pressure difference across the heat exchanger. The heat exchanger's primary side pressure is nearly atmospheric and the secondary side (power production) is pressurized to about 25MPa for supercritical cycle and 17MPa for subcritical cycle. Further in the analysis, the comparison of both the cycles will be carried out with recommendations.

1 INTRODUCTION

Next Generation Nuclear Reactors (NGNR) such as the Advanced High Temperature Reactor (AHTR) are intended to increase energy efficiency in the production of electricity and/or provide high temperature heat for industrial processes. Currently, the primary loop reference salt for AHTR is Li2BeF4, referred to as "Flibe." Heat in an AHTR is transferred from the reactor core by the primary liquid-salt coolant to an intermediate heat-transfer loop through intermediate heat exchangers (IHXs). The intermediate heat-transfer loop uses an intermediate liquid-salt coolant through a secondary heat exchanger (SHX) to move the heat to a power conversion system (Rankine cycle) as shown in Figure 1. The heat exchangers are considered key components that need to be extensively investigated because they are operated under a severe environment and their performance is directly related to the overall system efficiency and safety.

The AHTR have excellent safety attributes. The combined thermal capacity of the graphite core and the molten salt coolant pool offer a large time buffer to reactor transients. Compared to a light water reactor (LWR), AHTR should be more economical as illustrated by Ingresoll et al. (2004), because of higher power conversion efficiency, low pressure containment, and absence of active safety systems. The efficient transfer of energy for power production depends on the ability to incorporate effective heat exchangers between the nuclear heat transport system and the power production process. However, the need for efficiency, compactness, and safety challenge the boundaries of existing heat exchanger technology. Heat exchanger selection is most strongly influenced by the process application and operational conditions that determine or influence requirements for cost, size, reliability, robustness, maintenance, expected life, etc.

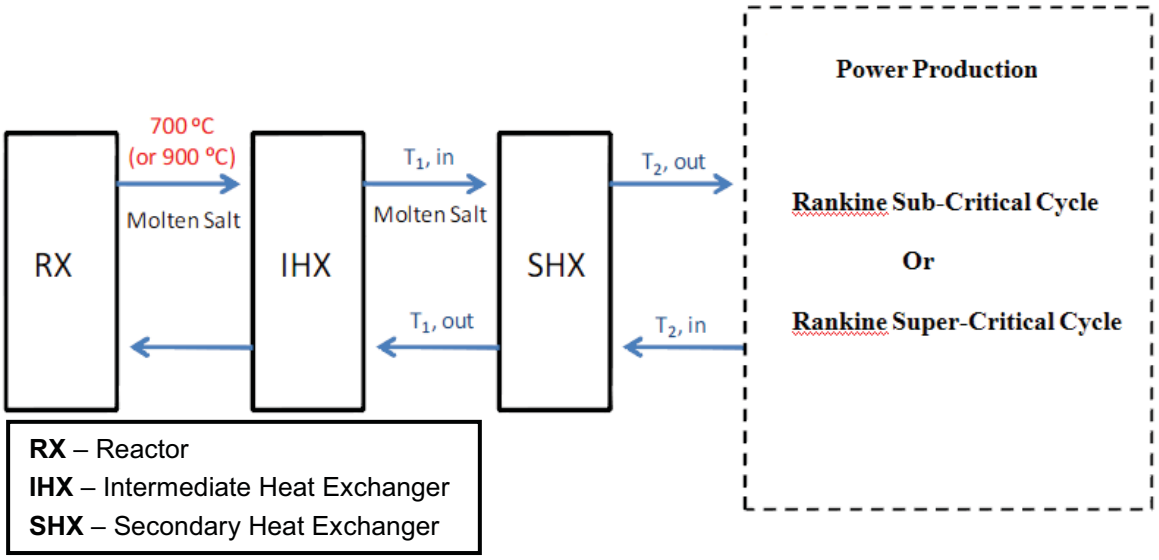

Figure 1. Thermal energy transfer for power production.

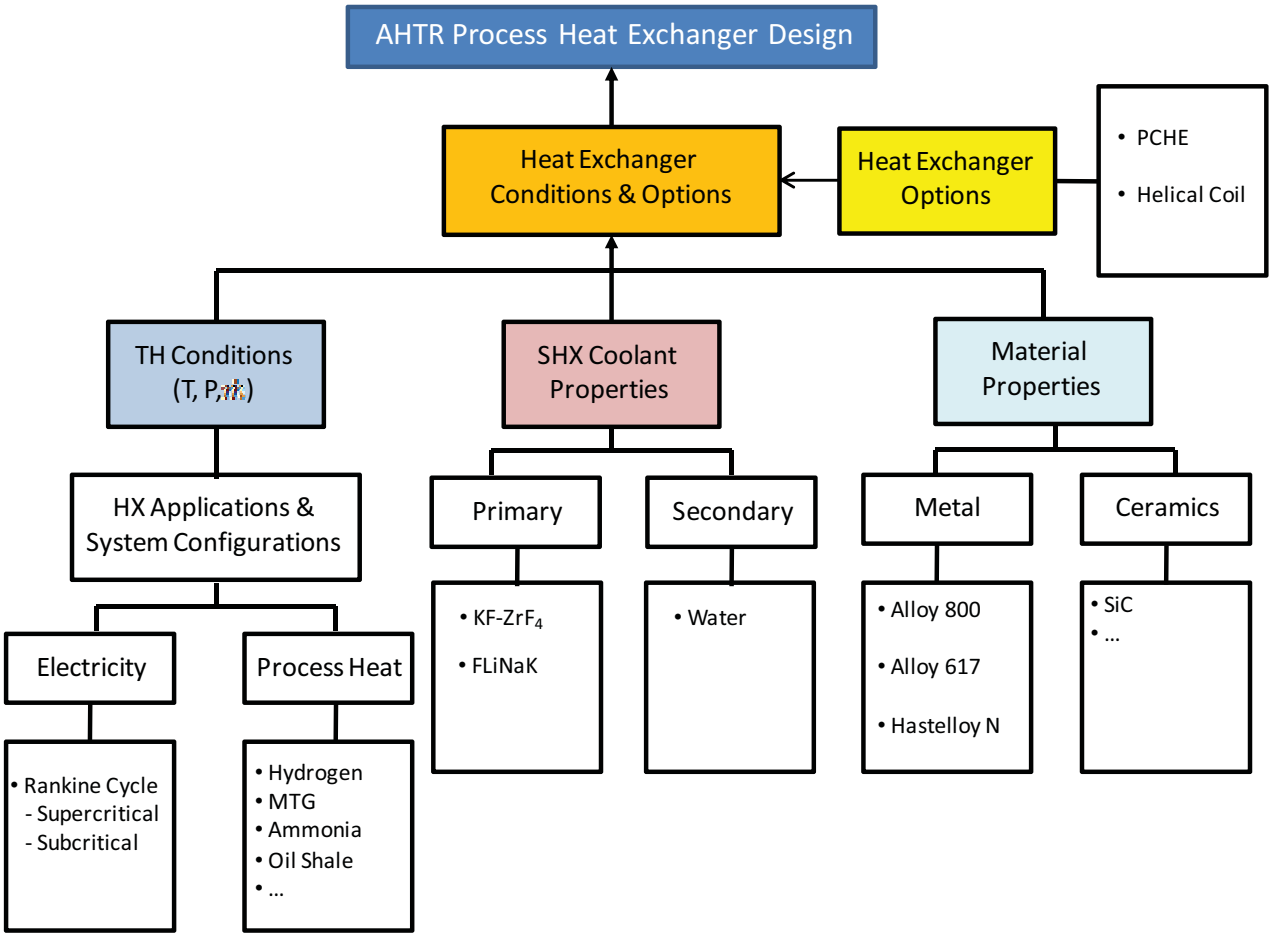

Figure 2. AHTR SHX heat exchanger design framework.

Table 1. SHX design requirements and basic conditions for the AHTR.

Parameter	Requirements
Reference System Configuration	AHTR + Supercritical Steam Rankine PCS:
Heat Exchanger Type	- Helical Coiled - Printed Circuit Heat Exchanger
Heat Exchanger Duty (MW)	3400
Primary Coolant	KF-ZrF_4
Secondary Coolant	Water/Steam
Primary Temperature (T_{in}/T_{out})	679/587°C (supercritical Rankine cycle) 679/586.1°C (subcritical Rankine cycle)
Secondary Temperature (T_{in}/T_{out})	251/593°C (supercritical Rankine cycle) 241.7/550°C (supercritical Rankine cycle)
Primary Pressure (MPa)	0.103
Secondary Pressure (MPa)	25 (supercritical Rankine cycle) 17.3 (subcritical Rankine cycle)
Tube Material	Hastelloy N
Shell Material	Hastelloy N

Irrespective of the type of heat exchanger, the performance of the heat exchanger is described by the heat transfer coefficient, friction factor relationships, and pressure drop. Operating the heat exchanger in the turbulent regime ensures higher flow rates, which does enhance the overall heat transfer coefficient but leads to a higher pressure drop. Ideally, the heat transfer coefficient should be as high as possible with lowest possible pressure drop. Having a lower pressure drop reduces the pumping cost while maintaining the requiredpressures downstream of the heat exchanger. Figure 2 presents a framework for AHTR process/secondary heat exchanger (SHX) selection and design that is dependent on the condition and environment of the application.

In this study, SHX thermal design for both supercritical and subcritical Rankine cycle is carried out. The thermal design of heat exchangers determines channel size, required length, and number of layers or tubes to meet a given thermal duty. The AHTR SHX design requirements and operating conditions are shown in Table 1. The heat exchanger of an AHTR is subjected to a unique set of conditions that impose several design challenges not encountered in standard heat exchangers. Corrosive molten salts, especially at temperatures in excess of 700°C, require specialized materials throughout the system to avoid corrosion. High steam pressures and high-temperatures create adverse material effects such as creep.

2 PRELIMINARY THERMAL DESIGN ANALYSES

This study provides a general description followed by thermal design analysis for both the helical coil heat exchanger and PCHE. The function of the process/SHX is to transfer heat from the secondary salt to the supercritical/subcritical Rankine cycle. Very high efficiency heat conversion is desired for the heat exchanger, as any heat that is not transferred to the process side reduces overall plant efficiency. PCHEs can provide significant reductions in volume and material usage. With tightly packed channels making adjacent streams able to effectively translate temperatures across their boundaries, approach temperatures (the difference between the outlet temperature of one fluid stream and the inlet temperature of the opposing fluid stream at their common header location) closer to 1°C are possible with compact heat exchangers. Shell-and-tube heat exchangers are often closer to 12°C in approach temperature, another demonstration of their inferior performance (Kandlikar et al. 2006).

The temperature difference between hot and cold fluids is continuously changing. Therefore, an effective difference needs to be calculated to determine heat flow through the wall separating the two fluids. This effective temperature difference is termed the Log Mean Temperature Difference (LMTD, ΔT_m). For the same inlet and exit temperature values of two fluids, ΔT_m attains a larger magnitude for countercurrent flow than the parallel flow, as explained by Singh (2004). Thus, the counterflow configuration is more effective in transferring heat than the parallel-flow arrangement and has been assumed for further thermal design in this study.

Two methodologies are commonly used to carry out thermal design for the heat exchanger: LMTD method, and Effectiveness – Number of Transfer Units ($\varepsilon - NTU$) method. Both methods are equivalent to each other. This analysis used the LMTD method. The analysis carried out here is appropriate for the preliminary design analysis (for scoping and comparison purposes). In order to make the design of a heat exchanger more manageable, the following assumptions were made for preliminary designs:

- The fluid properties are constant throughout the exchanger and are evaluated at the respective mean temperature
- Heat transfer coefficients of both sides are constant along the exchanger

- Flows in heat exchanger experience abrupt contractions at the entry and expansions at the exit, from the headers or ducts. In this analysis entry and exit losses are neglected
- Flow is assumed to be steady-state to avoid the complications of making transient calculations
- Two cases are individually analyzed:
  - Supercritical Rankine Cycle (25 MPa)
  - Subcritical Rankine Cycle (17 MPa).

A specified heat load ($\dot{Q}$), is given by the heat transfer and rate equations for either side as:

$$\dot{Q} = \dot{m}\, c_p \Delta T\,. \tag{1}$$

Rewriting the equation in terms of hot and cold fluids:

$$\dot{Q} = \dot{Q}_h = \dot{m}_h\, c_{p,h}\, (T_{h,in} - T_{h,out}) \tag{2}$$

and

$$\dot{Q} = \dot{Q}_c = \dot{m}_c\, c_{p,c}\, (T_{c,out} - T_{c,in})\,, \tag{3}$$

where Q_h is equal to Q_c, because the heat lost by the hot fluid is equal to the heat gained by the cold fluid. The product of $\dot{m}$ and c_p is called the heat capacity rate and is denoted by 'C'; the highest and lowest values of 'C' between hot and cold streams being 'C_{max}' and 'C_{min}'. If the ratio of C_{min} to C_{max} is unity, the exchanger is said to be balanced as explained by Hesselgreaves 2001.

The theoretically maximum possible heat exchanged between the hot and cold streams can be expressed as:

$$\dot{Q}_{max} = C_{min}\, (T_{h,in} - T_{c,in})\,, \tag{4}$$

which represents the idealized performance with infinite surface area, as explained by Hesselgreaves (2001). Maximum heat transferred is obtained when stream of lowest heat capacity rate has an outlet temperature equal to the inlet temperature (for a counterflow configuration) of the other stream. For parallel flow arrangements, this state is reached when both streams attain the same temperature at the outlet. In all cases, the state corresponds to a theoretically infinite surface area. The point of equal temperatures, called the pinch point, ideally corresponds to zero temperature difference, but in general it refers to the minimum temperature difference in the heat exchanger.

After defining the maximum possible heat transfer, heat exchanger effectiveness can be defined as

$$\varepsilon = \frac{\dot{Q}}{\dot{Q}_{max}} = \frac{C_h\,(T_{h,in} - T_{h,out})}{C_{min}(T_{h,in} - T_{c,in})} = \frac{C_c\,(T_{c,out} - T_{c,in})}{C_{min}(T_{h,in} - T_{c,in})} \tag{5}$$

where C_c and C_h are the cold and hot stream heat capacity rates.

The overall heat transfer coefficient is now determined followed by the calculation of LMTD. These values and the Q calculated above will finally be used to determine the surface area through which heat transfer takes place.

Heat exchanger performance is normally evaluated by the overall heat transfer coefficient U that is defined by the equation:

$$\dot{Q} = F(UA_s)\Delta T_m\,, \tag{6}$$

where, ΔT_m is the LMTD between the streams and *F* is a correction factor that depends on the flow configuration. UA_s is the product of the overall heat transfer coefficient and reference area, also known as heat transfer conductance. ΔT_m is calculated with the equation:

$$\Delta T_m = \frac{\Delta T_2 - \Delta T_1}{\ln\left(\frac{\Delta T_2}{\Delta T_1}\right)}\,, \tag{7}$$

where $\Delta T_2 = T_{h,out} - T_{c,out}$; $\Delta T_1 = T_{h,in} - T_{c,in}$.

Obtaining the respective values for $\dot{Q}$, overall heat transfer coefficient (U), and LMTD (ΔT_m),the size and number of plates/tubes were determined by solving for A_s. Dividing it further with inner cylinder's circumference could yield the required tube length needed for the heat exchanger for the given heat duty. Using this approach as a tool, the next section further discusses the preliminary design for both heat exchanger types.

2.1 Options for Heat Exchanger Types

Two different types of heat exchangers—helical coiled heat exchanger and printed circuit heat exchanger (PCHE)—are considered possible options for the AHTR SHX. The general features of these two candidate heat exchangers are described below.

2.1.1 Helical Coil Shell-and-Tube Heat Exchanger

Helical coil heat exchangers (HCHEs) are shell-and-tube type heat exchangers that consist of tubes spirally wound into bundles and fitted in a shell. The spiral geometry of the tubes transfer heat at a higher rate than straight tubes (Shah and Sekulic 2003). An HCHE is shown in Figure 3. Because of the tube bundle geometry, a considerable amount of surface can be accommodated inside the shell. These heat exchangers are used for gas-liquid heat transfer applications primarily when the operating temperature and/or pressure are very high. Cleaning a helical coil heat exchanger is very challenging (Shah and Sekulic 2003).

For the printed circuit heat exchanger, the primary and the secondary channels are geometrically identical andtherefore, the coolant type in each channel does not affect heat exchanger design. However, for HCHEs, design of the heat exchanger is significantly affected by selection of the coolant inside and outside of the tubes. Two options were evaluated for the HCHE design:

- Option 1: Tube (Molten Salt), Shell (Water/Steam)
- Option 2: Tube (Water/Steam), Shell (Molten Salt).

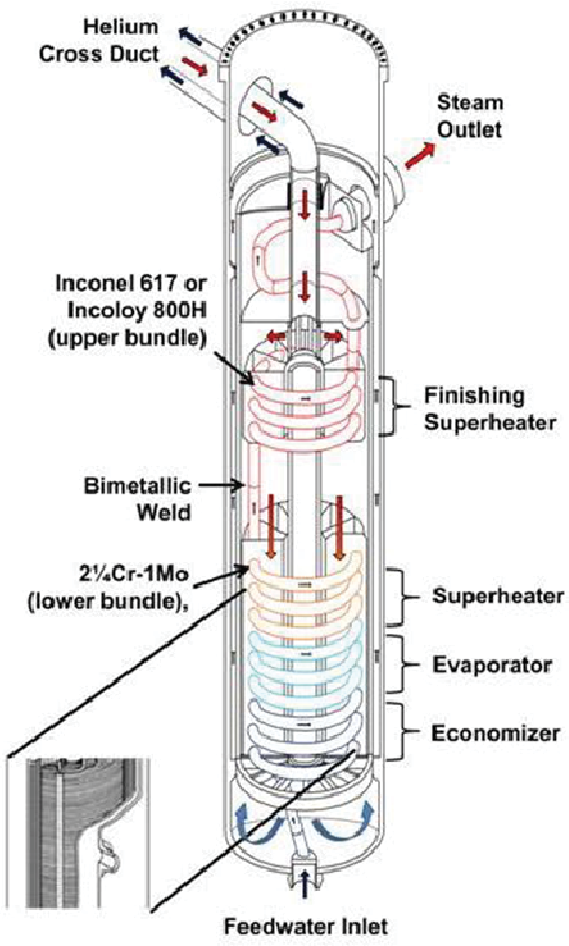

Figure 3. Helical coil heat exchanger

Preliminary Mechanical Design and Stress Analysis

Tables 2 and 3 show preliminary HCHE tube stress analysis results for both supercritical and subcritical Rankine cycles. In this stress analysis, tube and shell inner radius were assumed to be 0.0124 m and 1.65 m based on the intermediate heat exchanger (IHX) design for the high temperature test reactor (HTTR) in JAEA. While this heat exchanger transfers heat from helium to water, it was judged representative enough to compare Options 1 and 2. In this analysis, safety factors were assumed to be 1.0.

Table 2(A) shows the stress analysis and mechanical design calculations for Option 1 in the supercritical Rankine cycle. In this option, molten salt is inside the tubes and water/steam is on the shell side. Therefore, the tube is exposed to an external load and the shell is exposed to an internal load. According to the calculation, required minimum thickness for the tube is only 0.0016 m. However, the minimum thickness for the shell is 0.341 m, which is almost 15% of the vessel diameter. For larger safety factors and shell diameters, the required shell thickness will further increase, resulting in an unrealistic design. For this reason, Option 1 is not recommended.

Table 2(B) shows the stress analysis and mechanical design calculations for Option 2 where the molten salt is on the shell side and water/steam is inside the tubes. Therefore, the dominant load for both tube and shell is an internal load. However, the shell's inside pressure is from molten salt (200,000 Pa) and only marginally higher than the pressure outside (101,000 Pa). In this case the required minimum thickness for the tube and shell are estimated to be only 0.0014 m and 0.0015 m, respectively (for a safety margin of 1.0). Therefore, Option 2 is strongly recommended for the final design.

Tables 3(A) and 3(B) show similar results for the Subcritical Rankine Cycle. For this system, the recommended option is also Option 2, with molten salt on the shell side and water/steam inside the tubes. For this power cycle, the required minimum thickness for the tube and shell are estimated to be only 0.0012 m and 0.0015 m, respectively. Although the pressure (17.3 MPa) of the Subcritical Rankine Cycle is lower than the supercritical one (25 MPa), Option 1 still does not provide realistic mechanical design.

Table 2. Mechanical design of the tube and shell thicknesses (Supercritical Rankine).

(A) Option 1

Tube (Molten Salt)			Shell (Water/Steam)		
Parameter	unit	value	Parameter	unit	value
Tube inner radius	m	0.015	Shell inner radius	m	1.65
Tube inside pressure	Pa	100000	Shell inside pressure	Pa	24000000
Tube outside pressure	Pa	24000000	Shell outside pressure	Pa	100000
Yield stress (Hastelloy N)	Pa	217874000	Yield stress (Incoloy 800H)	Pa	129627000
max allowable stress	Pa	217874000	max allowable stress	Pa	129627000
tube minimum wall thickness	m	0.0016	Shell minimum wall thickness	m	0.341

(B) Option 2

Tube (Water/Steam)			Shell (Molten Salt)		
Parameter	unit	value	Parameter	unit	value
Tube inner radius	m	0.0124	Shell inner radius	m	1.65
Tube inside pressure	Pa	24000000	Shell inside pressure	Pa	200000
Tube outside pressure	Pa	100000	Shell outside pressure	Pa	100000
Yield stress (Hastelloy N)	Pa	217874000	Yield stress (Hastelloy N)	Pa	217874000
max allowable stress	Pa	217874000	max allowable stress	Pa	217874000
tube wall minimum thickness	m	0.0014	Shell minimum wall thickness	m	0.0015

Table 3. Mechanical design of the tube and shell thicknesses (Subcritical Rankine).

(A) Option 1

Tube (Molten Salt)			Shell (Water/Steam)		
Parameter	unit	value	Parameter	unit	value
Tube inner radius	m	0.015	Shell inner radius	m	1.65
Tube inside pressure	Pa	100000	Shell inside pressure	Pa	17300000
Tube outside pressure	Pa	17300000	Shell outside pressure	Pa	100000
Yield stress (Hastelloy N)	Pa	217874000	Yield stress (Incoloy 800H)	Pa	129627000
max allowable stress	Pa	217874000	max allowable stress	Pa	129627000
tube minimum wall thickness	m	0.0013	Shell minimum wall thickness	m	0.247

(B) Option 2

Tube (Water/Steam)			Shell (Molten Salt)		
Parameter	unit	value	Parameter	unit	value
Tube inner radius	m	0.0124	Shell inner radius	m	1.65
Tube inside pressure	Pa	17300000	Shell inside pressure	Pa	200000
Tube outside pressure	Pa	100000	Shell outside pressure	Pa	100000
Yield stress (Hastelloy N)	Pa	217874000	Yield stress (Hastelloy N)	Pa	217874000
max allowable stress	Pa	217874000	max allowable stress	Pa	217874000
tube wall minimum thickness	m	0.0012	Shell minimum wall thickness	m	0.0015

Preliminary Thermal Design Analysis

Previously, a general methodology for determining the heat transfer surface area was presented. The following equations were used to expand on the calculation for A_s to determine tube dimensions and other details for the HCHE:

Radius of tube:

$$a = \frac{d_i}{2} \tag{8}$$

where,

$d_i -$ *tube inner diameter*

$d_o -$ *tube outer diameter* $= (d_i + 2 * t_h)$

$t_h -$ *tube thickness*

Radius of curvature:

$$R_{eff} = \frac{(R_{in} + R_{out})}{2} \tag{9}$$

Number of tubes in the bundle:

$$N_{tb} = \frac{(R_{out} - R_{in})}{p} * \frac{L_m}{p} \tag{10}$$

where,

R_{out} – *shell outer radius* (*assumed value*: $3.5m$)

R_{in} – *shell inner radius* (*assumed value*: $1.5m$)

L_m – *tube bundle length* (*assumed value*: $1.0m$)

p – *tube pitch* (*assumed value*: $0.05m$)

Nusselt number for straight pipe (Dittus-Boelter (Kays and Crawford 1981)):

$$Nu_0 = 0.022\left(Re_t^{0.8}\right)\left(Pr_t^{0.5}\right) \tag{11}$$

Nusselt number for Helical Coil (Shah et al. 1987):

$$Nu_t = Nu_0\left\{1.0 + 3.6\left[1 - \left(\frac{a}{R_{eff}}\right)\right] * \left(\frac{a}{R_{eff}}\right)^{0.8}\right\} \tag{12}$$

Therefore, the heat transfer correlation inside the tube can be estimated as follows:

$$h_t = Nu_t \frac{K_{tube}}{d_i} \quad (13)$$

Where, K_{tube} – thermal conductivity of the tube material

In the tube side, heat transfer correlations are based on the heat transfer in inline tube bundles in smooth pipes.

To estimate the heat transfer in the inline tube bundles, some parameters -such as the correction factor for the tube rows and the Prandtl number for the tube wall are defined as:

Correction factor (C): 1 (for large number of tubes)

Prandtl number for the tube wall: $Pr_s = Pr_w$ (Prandtl number for the tube wall was assumed to be the same as the bulk phase)

Nusselt number for the shell side can be estimated as follows (Zukauskas, 1987):

$$Nu_s = \left\{0.9\, C * (Re_s^{0.4})(Pr_s^{0.36})\left(\frac{Pr_s}{Pr_w}\right)^{0.25} \; for\; Re_s < 10^2\right\}$$
$$\left\{0.52\, C * (Re_s^{0.4})(Pr_s^{0.36})\left(\frac{Pr_s}{Pr_w}\right)^{0.25} \; for\; 10^2 < Re_s < 10^3\right\}$$
$$\left\{0.27\, C * (Re_s^{0.63})(Pr_s^{0.36})\left(\frac{Pr_s}{Pr_w}\right)^{0.25} \; for\; 10^3 < Re_s < 2 * 10^5\right\}$$
$$\left\{0.033\, C * (Re_s^{0.8})(Pr_s^{0.4})\left(\frac{Pr_s}{Pr_w}\right)^{0.25} \; for\; 2 * 10^5 < Re_s < 2 * 10^6\right\} \quad (14)$$

Therefore, the heat transfer correlation on the shell side can be estimated as follows:

$$h_s = Nu_s \frac{K_{shell}}{d_o} \quad (15)$$

Where K_{shell} – thermal conductivity of the shell material

Since the tube thickness is small, the effect of heat transfer resistance at the wall has been neglected.

Overall Heat Transfer Coefficient:

$$U = \frac{1}{\frac{1}{h_t} + \frac{1}{h_s}} \quad (16)$$

Heat Transfer Surface Area:

$$A_s = \frac{Q}{U * \Delta T_m} \quad (17)$$

Tube Length:

$$Lt_{middle} = \frac{A_s}{\pi\left(\frac{d_i + d_o}{2}\right) * N_{tb}} \quad (18)$$

Number of rotations of the tube bundle:

$$N_b = \frac{Lt_{middle}}{\pi\,(R_{in} + R_{out})} \quad (19)$$

Therefore, Shell Length can be calculated as:

$$L_s = L_m * N_b \quad (20)$$

After establishing tube dimensions and parameters in this manner, pressure drop inside the tube can be estimated by the following equation (Kakac. S., Shah, R., and Aung, W., 1987):

Tube side

Friction factor inside the Helical Coiled Tubes:

$$f = \left[0.0084\left[Re_t\left\{\frac{\left(\frac{R_{in}+R_{out}}{2}\right)}{a}\right\}^{-2}\right]^{-0.2}\left\{\frac{\left(\frac{R_{in}+R_{out}}{2}\right)}{a}\right\}^{-0.5}\right] \quad (21)$$

Pressure drop inside the Helical Tube:

$$\Delta P_{tube} = 4 * f * \left(\frac{Lt_{middle}}{d_i}\right) * \rho_{tube} * \frac{V_t^2}{2} \quad (22)$$

where,

V_t – *coolant velocity in the tube side*

ρ_{tube} – *density of the coolant in the tube*

Shell side

$$p_{ratio} = \frac{p}{d_o} \quad (23)$$

Hagen Number for Inline Tube Bundles (Martin, 2002)

$$Hg_{laminar} = \frac{140 * Re_s\left(p_{ratio}^{0.5} - 0.6\right)^2 + 0.75}{\left[p_{ratio}^{1.6}\left(\frac{4 * p_{ratio} * p_{ratio}}{\pi} - 1\right)\right]} \quad (24)$$

$$Hg_{turbulent} = \left\{\left[0.11 + \frac{0.6 * \left(1 - \frac{0.94}{p_{ratio}}\right)^{0.6}}{(p_{ratio} - 0.85)^{1.3}}\right] * 10^{0.47 * (-0.5)} + 0.015 *\right.$$
$$\left. pratio - 12 * Res1.9\right. \quad (25)$$

$$Hg = Hg_{laminar} + Hg_{turbulent} \quad (26)$$

Number of Effective Tube Bundles:

$$N_{tb} = N_b * \left(\frac{L_m}{p}\right) \quad (27)$$

Therefore, pressure drop on the shell side is as follows:

$$\Delta p_{shell} = \frac{\mu_{shell}^2}{\rho_{shell}} \frac{N_{tb}}{d_o^2} * \mathrm{Hg} \quad (28)$$

Table 4 shows the preliminary thermal design for the helical coil heat exchanger for Supercritical and Subcritical Rankine Cycle respectively.

Table 4. Preliminary design specifications for secondary heat exchanger (helical coiled) for Subcritical and Supercritical Rankine Cycle.

Specification	Unit	Supercritical Rankine Cycle- SHX	Subcritical Rankine Cycle-SHX
Heat Duty	MW(t)	3400	3400
Number of Units	-	1	1
Primary coolant (Shell)	-	Molten Salt	Molten Salt
Secondary coolant (Tube)	-	Water/Steam	Water/Steam
Primary inlet T	◦C	679	679
Primary outlet T	◦C	587	586.1
Secondary inlet T	◦C	251	241.7
Secondary outlet T	◦C	593	550
Primary pressure (Shell)	MPa	0.1	0.1
Secondary pressure (Tube)	MPa	24	17.3
Tube diameter	m	0.03	0.03
Tube pitch	m	0.05	0.05
Tube thickness	mm	1.4	1.24
Number of tubes	-	740	740
Number of tube rotations	-	4.12	3.33
Tube material	-	Hastelloy N	Hastelloy N
Shell inside diameter	m	3.3	3.3
Shell outside diameter	m	7	7
Shell material	-	Hastelloy N	Hastelloy N
Overall heat transfer coefficient	W/m K	3804.16	3959.51
Heat transfer surface area	m^2	4871.922	3914.71
Pressure drop in shell	kPa	15.61	11.66
Pressure drop in tube	kPa	36.3	52.57

2.1.2 Printed Circuit Heat Exchanger

The Printed Circuit Heat Exchanger (PCHE) is a relatively new concept, as shown Figure 4, that has been commercially manufactured by Heatric™ since 1985. PCHEs are robust, combining compactness, low pressure drop, high effectiveness, and the ability to operate with a very large pressure differential between hot and cold sides (Heatric™ Homepage 2011). These heat exchangers are especially well suited to applications where compactness is important. As the name implies, PCHEs are manufactured by the same technique used to produce standard printed circuit boards for electronic equipment. Individual plates are etched to produce channels. These etched plates are thereafter joined by diffusion welding, resulting in extremely strong all-metal heat exchanger cores. The diffusion welding process includes a thermal soaking period to allow grain growth across the joint and between the plates, which creates a joint with nearly the same strength as the base material. Hence, the joint has very high pressure containment capability and avoids the creation of corrosion cells observed in traditional welding, as explained by Hesselgreaves (2001). The fluid passages are semicircular in cross-section, typically being 1.0 to 2.0 mm wide and 0.5 to 1.0 mm deep with a hydraulic diameter of 1.5 to 3 mm (Hesselgreaves 2001). After bonding, any number of core blocks can be welded together to provide the required flow capacity.

Figure 4. Printed circuit heat exchanger (Heatric™ homepage 2011).

The thermal design of printed circuit heat exchangers is subjected to very few constraints. Fluids may be liquid, gas or two-phase, multistream and multipass configurations can be assembled and flow arrangements can be truly counter-current, co-current or cross-flow, or a combination of these, at any required pressure drop.

Where required, high heat exchange effectiveness (over 98%) can be achieved through very close temperature approaches in counter-flow. To simplify control or further maximize energy efficiency, more than two fluids can exchange heat in a single core. Heat loads can vary from a few watts to many megawatts, and these exchanger's can weigh from a few kilograms to thousands of kilograms.

Flow induced vibration, an important source of failure in shell-and-tube exchangers, is largely absent from printed heat exchangers.

Thermal Design Guideline and Constraints

A worskshop held by MIT and Heatric in 2003 was reported by Gezelius 2004 in his thesis, which includes the summary of the workshop in 2003 between MIT and Heatric. In this part, we summarized the guidelines and criteria for designing the PCHE for IHX (Sabharwall et al, 2011):

- No gasket or brazing (risk of leak is considerably reduced): two orders of magnitude lower
- Very low vibration damage
- No fouling under clean gas conditions
- Surface area density: about 2,500 m^2/m^3
- No heat transfer and friction factor correlations are available
- Semi-circular cross-section
- Width: 1.0–2.0 mm (2.0 mm shows maximum thermal performance and economic efficiency but for nuclear application, 1.2 mm is suggested.)
- Depth: 0.5–1.0 mm
- Weight based costing: $30/kg for stainless steel, $120/kg for titanium, expected to be less than $40/kg for nuclear application (not known for Hastelloy N)
- Carbon steel is typically not used because of the small channel diameter vulnerable to corrosion and unsuitability for diffusion bonding.
- Average mass-to-duty ratio: 0.2 tones/MW (13.5 tones/MW in shell-and-tube design)
- No constraint to the pressure drop
- Multiport Printed Circuit Heat Exchanger module size: width: 0.5m (1.5m is max), height: 0.6 m, depth: 0.4~0.6 m.
- Fatigue can be caused by thermal transient.
- Only pressure drop restrict the velocity.
- Estimated minimum life ~ 20 years.

Preliminary Thermal Design Analysis

In this study, two adjacent hot channels are assumed for each cold channel in the PCHE as shown in Figure 5.

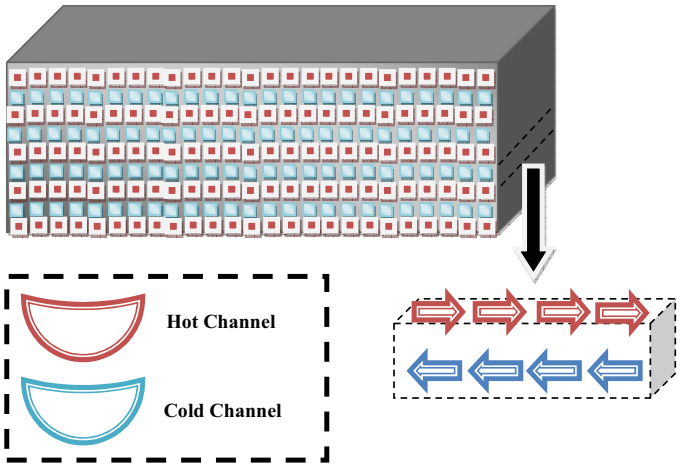

Figure 5. Detail description for PCHE (counter flow arrangement).

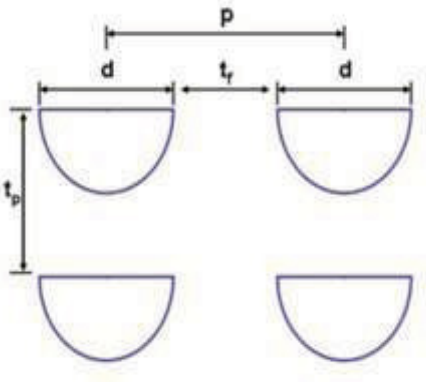

Figure 6. Channel arrangement of PCHE (Sabharwall et. al, 2011).

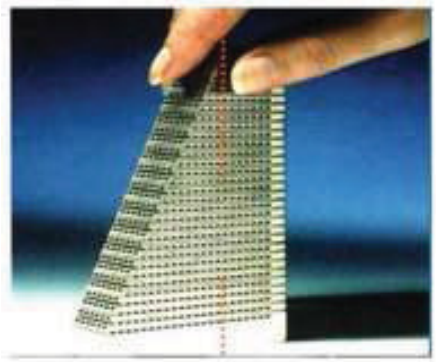

Figure 7. PCHE (Heatric™ homepage 2011).

Figure 6 and 8 shows the channel arrangement and the schematic of PCHE. Using the general methodology for the

thermal deign presented in section 2, the following equations were used for the printed circuit heat exchanger design:

Heat exchanger geometrical parameters (Kim et al. (2008), Hesselgreaves (2001)):

:

Channel horizontal distance:

$$t_f = p - d \tag{29}$$

Ratio of free flow area to frontal area:

$$\sigma = \frac{\frac{1}{2}*\frac{\pi}{4}*d^2}{(d+t_f)*t_p} \tag{30}$$

Effective diameter:

$$d_e = \frac{4*\frac{\pi}{8}*d^2}{\frac{\pi*d}{2}+d} \tag{31}$$

Heat Transfer Coefficient:

In this section, heat transfer for the compact heat exchanger is estimated, in this thermal design study the channel is assumed to be straight throughout the flow paths, (Dittus and Boelter (1930)),

$$\begin{aligned} Nu_h &= 3.657, \quad if\ Re_h < 2300 \\ &= 0.023 * Re_h^{0.8} *, Pr_h^{0.33} \ \ if\ Re_h > 2300 \\ Nu_c &= 3.657, \quad if\ Re_c < 2300 \\ &= 0.023 * Re_c^{0.8} *, Pr_c^{0.4} \ \ if\ Re_c > 2300 \end{aligned} \tag{32}$$

where $Nu_h\ and\ Nu_c$ are the hot side and cold side Nusselt numbers. The Reynolds numbers, $Re_h\ and\ Re_c$, are based on the effective diameters of the and the respective hot side and cold side Reynolds numbers.

From the above equation, the convective heat transfer coefficient can be calculated as:

$$h_h = Nu_h\ \frac{K_h}{d_e};\ \ h_c = Nu_c\ \frac{K_c}{d_e} \tag{33}$$

and the Overall Heat Transfer Coefficient can be calculated as:

$$U = \frac{1}{\frac{1}{h_h}+R_w+\frac{1}{h_c}} \tag{34}$$

where R_w is the resistance in heat transfer wall $\left(R_w = \frac{t_f}{K_{wall}}\right)$.

Heat Transfer Surface Area:

$$A_s = \frac{Q}{U*\Delta T_m} \tag{35}$$

Number of channels on the hot and cold side, respectively:

$$N_h = \frac{A_h}{\left(\frac{\pi}{8}\right)*d^2} \tag{36}$$

$$N_c = \frac{A_c}{\left(\frac{\pi}{8}\right)*d^2} \tag{37}$$

Heat Exchanger Channel length for hot and cold side:

$$Length_h = \frac{A_s}{\left(\frac{\pi}{2}*d+d\right)*N_h} \tag{38}$$

$$Length_c = \frac{A_s}{\left(\frac{\pi}{2}*d+d\right)*N_c*2} \tag{39}$$

After establishing channel dimensions and parameters in this manner, the pressure drop inside the channnel can be estimated by the following equation (Idelchik, 1986):$f_{ht}(x) = \frac{1}{\sqrt{x}} - 4 *$ $(\log\left(Re_h\sqrt{x}\right) - 0.40)$ (40)

$$\begin{aligned} f_h &= \frac{16}{Re_h} \ \ if\ Re_h < 2300 \\ &= root(f_{ht}(x), x, 1)\frac{16}{Re_h} \ \ if\ Re_h \geq 2300 \end{aligned}$$

Therefore, pressure drop in the hot channel can be estimated as:

$$\Delta P_h = 4 * f_h * \frac{Length_h}{d_e} * \ \rho_h * \frac{V_h^2}{2} \tag{41}$$

Similarly for the cold side,

$$\begin{aligned} f_{ct}(x) &= \frac{1}{\sqrt{x}} - 4 * (\log\left(Re_c\sqrt{x}\right) - 0.40) \\ f_c &= \frac{16}{Re_c} \ \ if\ Re_c < 2300 \\ &= root(f_{ct}(x), x)\frac{16}{Re_c} \ \ if\ Re_c \geq 2300 \end{aligned} \tag{42}$$

Therefore, pressure drop in the hot channel can be estimated as:

$$\Delta P_c = 4 * f_c * \frac{Length_c}{d_e} * \ \rho_c * \frac{V_c^2}{2} \tag{43}$$

Where,
f_h friction factor for the hot side
f_c friction factor for the cold side

V_h and V_c is the coolant velocity in the hot and cold channel respectively.

Table 5 shows the preliminary thermal design for the printed circuit heat exchanger for supercritical and sub critical Rankine cycles, respectively.

Table 5. Preliminary design specifications for secondary heat exchanger (PCHE for Subcritical and Supercritical Rankine Cycle).

Specification	Unit	Supercritical Rankine Cycle- SHX	Subcritical Rankine Cycle-SHX
Heat Duty	MW(t)	3400	3400
Number of Units	—	1	1
Primary coolant (primary)	—	Molten Salt (KFZr4)	Molten Salt (KFZr4)
Secondary coolant (secondary)	—	Water/Steam	Water/Steam
Primary inlet T	◦C	679	679
Primary outlet T	◦C	587	586.1
Secondary inlet T	◦C	251	241.7
Secondary outlet T	◦C	593	550
Primary pressure	Pa	1.00E+05	1.00E+05
Secondary pressure	Pa	2.40E+07	1.73E+07
Channel diameter	m	0.003	0.003
Channel pitch	m	3.33E-03	3.24E-03
Plate thickness	m	3.17E-03	3.17E-03
Number of total primary channels	—	3678247	3678247
Number of total secondary channels	—	1839123	1839123
Module width	m	0.6	0.6
Module height	m	0.6	0.6
Module length	m	0.85	0.7
Overall Heat Transfer Coefficient	W/m K	1500.55	1552.76
Primary pressure drop	kPa	18.4	14.82
Secondary pressure drop	kPa	0.86	1.21

3 SUMMARY AND CONCLUSIONS

Preliminary heat exchanger design has been performed in this study. The AHTR secondary heat exchanger transfers heat from the molten salt intermediate loop to the power conversion system based on steam Rankine cycles. The total thermal requirement of the heat exchanger is 3400 MWt. HCHEs and PCHEs were determined to be the possible heat exchanger options capable of satisfying design requirements.

A simple stress analysis was used for determining tube and shell thicknesses of the HCHEs, and for determining channel pitch and plate thickness of the PCHEs. As a result, it was concluded that for HCHEs, the coolant inside the tube is water/steam and the shell side coolant is molten salt.

A simple thermal design method was used for determining overall design specifications including geometry, sizing, and configurations. Tables 4 and 5 summarize the design specifications for helical coiled heat exchangers and PCHEs, respectively. Mainly, for the same heat duty helical coil heat exchanger showed 2.5 times higher overall heat transfer coefficient, but also had a much higher pressure drop when compared with the printed circuit heat exchanger. Further experiments should be carried out for validation and for overall uncertainty quantification.

ACKNOWLEDGMENTS

This submitted manuscript was authored by a contractor of the U.S. Government under DOE Contract No. DE-AC07-05ID14517. Accordingly, the U.S. Government retains and the publisher, by accepting the article for publication, acknowledges that the U.S. Government retains a nonexclusive, paid-up, irrevocable, world-wide license to publish or reproduce the published form of this manuscript, or allow others to do so, for U.S. Government purposes.

REFERENCES

AREVA, *NGNP with Hydrogen Production IHX and Secondary Heat Transport Loop Alternatives*, 12-9076325-001, 2008.

Dittus, P. W., and L. M. K. Boelter, Univ. Calif. Pub. Eng., Vol. 2, No. 13, pp. 443-461 (1930), reprinted in Int. Comm. Heat Mass Transfer, Vol. 12, pp. 3-22 (1985), 1930.

Heatric, 2011, *General heat exchanger overview*, http://www.heatric.com/diffusion_bonded_exchangers.html, visited 9/22/2011.

Hesselgreaves, J.E., "Compact Heat Exchangers: Selection, Design and Operation", Pergamon Press, 2001.

Idelchik, I.E., and Fried, E., Handbook of hydraulic resistance: second edition, Hemisphere Publishing, New York, NY, 1986.

Ingersoll, D. T., C. W. Forsberg, L. J. Ott, D. F. Williams, J. P. Renier, D. F. Wilson, S. J. Ball, L. Reid, W. R. Corwin, G. D. Cul, P. F. Peterson, H. Zhao, P. S. Pickard, E. J. Parma, and M. Vernon, 2004, "Status of Preconceptual Design of the Advanced High-Temperature Reactor (AHTR)," ORNL/TM-2004/104, May 2004.

Kakac, S., Liu, H., 2002, *Heat Exchangers: Selection, Rating, and Thermal Design*, CRC Press, ISBN 0-8493-0902-6.

Kandlikar, S. G., Garimella, S., Li, D., Colin, S., & King, M. R., "Heat Transfer and Fluid FLow in Minichannels and Microchannels*",* Kidlington, Oxford: Elsevier Ltd, 2006.

Kays, W.M., and Crawford, M.E., "Convective Heat and Mass Transfer," McGraw-Hill, 2nd Edition, New York, 1981.

Kim, E.S., Oh, C.H., Sherman, S., Simplified optimum sizing and cost analysis for compact heat exchanger in VHTR, Nuclear Engineering and Design, Vol. 238, pp. 2635-2647, 2007.

Martin, H., "The generalized Leveque equation and its practical use for the prediction of heat and mass transfer rates from pressure drop," Chemical Engineering Science, 57, pp 3217-3223, 2002.

Sabharwall, P., Kim, E.S., Siahpush, A., Anderson, N.A., Glazoff, M., Phoenix, W., Mizia, R., Clark, D., McKellar, M., and Patterson, M., "Feasibility Study of Secondary Heat Exchanger Concepts for the Advanced High Temperature Reactor," *External Report*, INL/EXT-11-23076, Idaho National Laboratory, Idaho, September 2011.

Shah, R.K., and Joshi, S. D., "Convective Heat Transfer in Curved Pipes in Handbook of Single-Phase Convective Heat Transfer," Kakac, S., Shah, R.K., and Aung, W., John Wiley &Sons, New York, Ch 5, 1987.

Shah, R. K., & Sekulic, D. P., "Fundamentals of Heat Exchanger Design"*,* Hoboken, NJ: John Wiley & Sons, 2003.

Singh, P. P. 2004, "Thermal Design of Heat Exchangers." *Encyclopedia of Agricultural, Food, and Biological Engineering*, Ed: D. R. Heldman, Marcel Dekker, NY.

Zukauskas, A. A., 1987, "Convective Heat Transfer in Cross Flow," in *Handbook of Single-Phase Convective Heat Transfer*, Kakac, S., Shah, R. K., and Aung, W., Eds., John Wiley & Sons, New York, 1987, Ch.5.